# GeoSciences 2014

Annual Conference of the Geoscience Society of New Zealand

Field Trip 5

28th November 2014

# FROM SUMMIT TO SWAMP: HIGH AND LOW EXPLOSIVE ERUPTIVE RECORDS AT MT TARANAKI

**Rafael Torres-Orozco[1], Maggi Damaschke[1] and Alan Palmer[2]**

[1]Volcanic Risk Solutions and [2]Department of Soil and Earth Sciences, Massey University, Private Bag 11222, Palmerston North

**Cover photo:** Deposits of explosive pyroclastic eruptions exposed on the flanks of Mount Taranaki. Photo R. Torres-Orozco.

## Bibliographic reference:

Torres-Orozco, R., Damaschke, M., Palmer, A. (2014). From summit to swamp: high and low explosive eruptive records at Mt Taranaki. In: Holt, K.A. (compiler). Field Trip Guide Volume, GeoSciences 2014 Conference, 24th – 27th November 2014, Pukekura Raceway and Function Centre, New Plymouth, New Zealand. Geoscience Society of New Zealand Miscellaneous Publication 139B. pp 5 - 14.

# Field Trip Outline

8 am: Depart conference venue, Pukekura Raceway, New Plymouth, and travel to Dawson Falls car-park via the southeastern entrance of Egmont National Park. Tramp to stop 1.

**STOP 1**: **Wilkies Pools section 1**

- View of channel-facies Pyroclastic Density Current (PDC) deposits of the ca. 2 kyr BP Maketawa 2 eruptive unit.

**STOP 2: Wilkies Pools section 2**

- Post ca. 5 kyr BP proximal stratigraphy: main-axis and marginal-facies PDC and fallout deposits of Tariki, Mangatoki, Korito, Upper Inglewood, and Manganui eruptive units.
- Tramp to next section.

**STOP 3: Stratford Plateau section**

- Lateral transitions of PDC and fallout deposits: Maketawa 2, Manganui, and Upper Inglewood eruptive units and subunits.
- Tramp to Stratford Plateau car-park.

**STOP 4: Stratford Plateau car-park and Curtis Ridge section**

- Short tramp to Curtis Ridge Section: Main section for Manganui and Upper Inglewood eruptive units, subunits, and facies transitions. View and transitions of <2 kyr BP "high- and low-explosive" proximal records.
- Core-Drilling explanation with cores obtained from swamps outside Egmont National Park.

**STOP 5: New Stratford Plateau section**

- Transitions of deposits observed at Curtis Ridge Section: Maketawa 1 and 2, Manganui units, Upper Inglewood, and Korito eruptive unit.

**STOP 6: Upper Pembroke Road section**

- Proximal-longitudinal transitions of Manganui and Upper Inglewood units.

**STOP 7: Lower Pembroke Road section**

- Medial-longitudinal transitions of Manganui and Upper Inglewood units.

## Introduction

New Zealand's hazardscape is well recognized for its recurrent explosive volcanic activity. The Taupo Volcanic Zone (TVZ) is typically the centre of attention, as it is the source of some of the largest and environmentally disruptive Quaternary rhyolithic ignimbrites ever recorded in Earth's geological history, of up to 1000 $km^3$ (Wilson et al., 1995; Wilson, 1997; Manville et al., 2009). However, notable historical examples of highly explosive eruptions at andesitic volcanoes such as 79 AD Mt. Vesuvius (Carey and Sigurdsson, 1987), 1980 Mt. St. Helens (Tilling et al., 1990), 2008 Chaiten (Carn et al., 2009), 2010 Eyjafjallajökull eruption (Gudmundsson and Pedersen 2010; Langmann et al., 2012), and 2010 Merapi (Cronin et al., 2013); have demonstrated that sub-plinian and plinian events of orders of magnitude and volumes (ca. 0.1-1 $km^3$) less than rhyolitic eruptions are able to cause equally significant damage to the human and environmental realms.

Little is known about the largest explosive eruptions at andesitic volcanoes in New Zealand (NZ). Recently, Pardo et al. (2012a; 2012b) calculated minimum volumes of 0.6 $km^3$ for the five <27 kyr BP largest eruptions at Mt. Ruapehu. Platz et al. (2007) estimated a volume of 0.3 $km^3$ for the most recent sub-plinian event at Mt. Taranaki - the Burrell eruption (comprising the 1655 AD Burrell Lapilli; Druce, 1966; Neall, 1972). These plinian events involved eruptive columns of up to 37 km high, which dispersed air fall ash and pumice over the North Island of NZ; as well as pyroclastic density currents of lower volumes (ca. 0.001-0.01 $km^3$) and more restricted distributions (limited to near National Park areas in both cases) but never-the-less, still highly disruptive.

The aim of this fieldtrip is to provide a lithostratigraphic overview of different pyroclastic deposits produced during the largest eruptions at andesitic volcanoes, using Mt. Taranaki as the perfect example of this type. We will visit south-eastern and eastern proximal sections which expose the most detailed deposits of the largest <5 kyr BP events at Mt. Taranaki; spanning not only highly explosive phases, but also including intervening periods of low-explosive activity. This will demonstrate the full multiphase eruption episode or cycle. In addition, we will observe drilled sediment cores of pyroclasts deposited in swamps, collected from outside the National Park, which mostly correspond to medial-distal deposits of the largest events. Such records provide an important source of data to understand how eruptions were distributed, and to obtain a longer time frame of the eruptive history of the volcano.

## Fieldtrip area

Mt. Taranaki (also known as Mt. Egmont) is the largest andesite stratovolcano in NZ. It consists of a 2518 m high volcanic edifice of 25 $km^2$ and 12 $km^3$, and a relatively flat surface of 1000 $km^2$ and 150 $km^3$ termed the volcanic ring-plain (Neall et al., 1986; Zernack et al., 2011; Fig. 1). Lava flows of ca. 8 kyr BP (Warwicks Castle Group; Neall, 1979; Stewart et al., 1996) constitute the core of the present-day volcanic edifice. Some of the youngest blocky lava flows on the northern and southern sides of the cone can be traced up to the west-breached crater rim. Inside the crater, remnants of the ca. 1800 AD half-collapsed Sisters dome make up the summit (Platz et al., 2012). The ca. 7 kyr BP, 1962 m high, Fanthams Peak parasitic cone (Stewart et al., 1996) breaks the nearly perfect cone-shaped symmetry of Mt. Taranaki on its southern flank. The ring-plain is composed of extensive, coalescing fans of volcanic and volcaniclastic sequences that were deposited during the last ca. 130 kyr BP, and extend beyond the current coastline (Alloway et al., 2005). Its near-circular outline is broken to the

north-northwest by Pouakai and Kaitake volcanoes, to the north by a dissected Pleistocene laharic surface, and to the east by hills of eroded Tertiary marine sediments (Neall and Alloway, 2004).

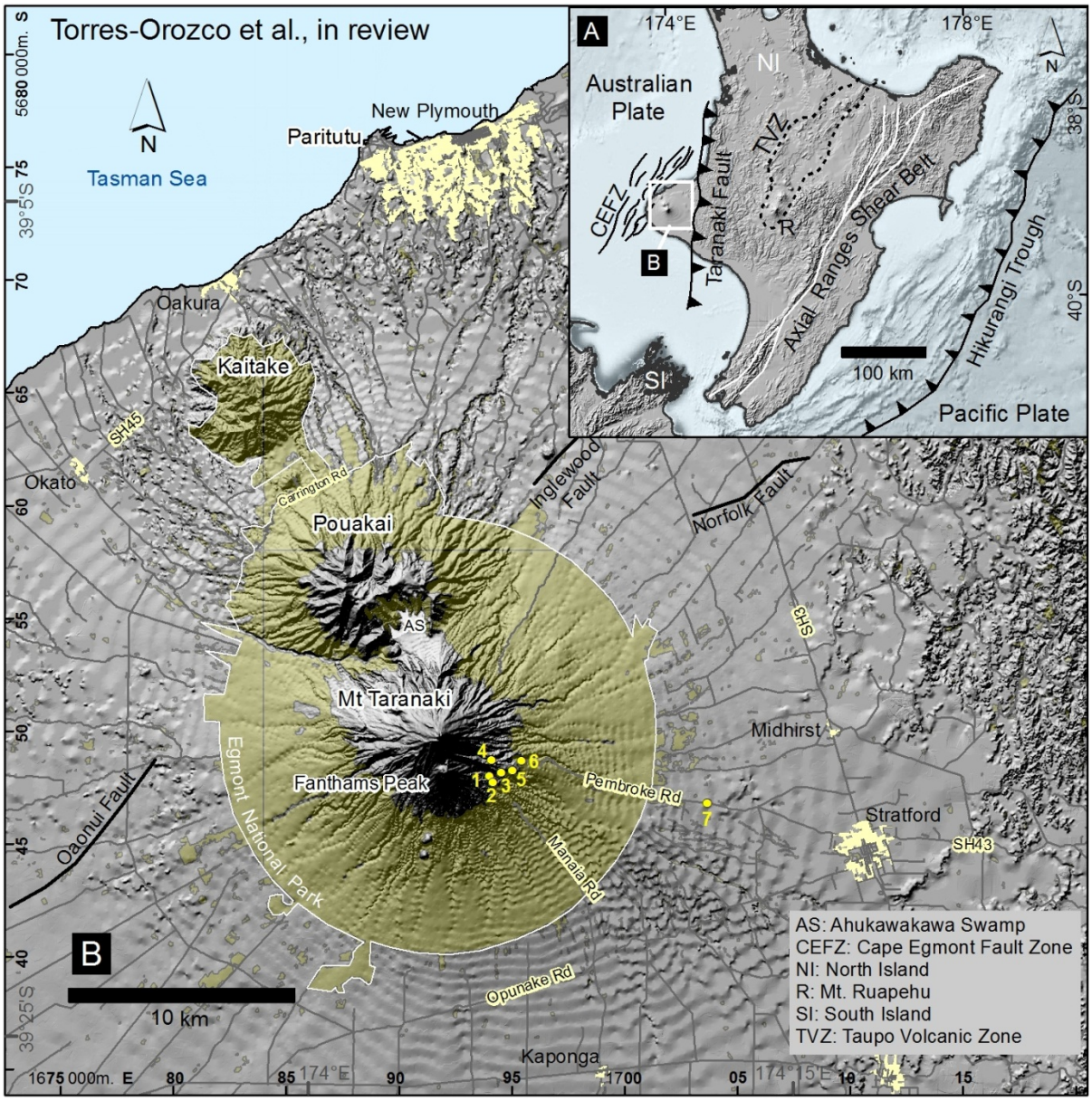


Figure 1. Location of Mt. Taranaki and stops.

## Volcanic history of Mt. Taranaki

The volcanic history of the ca. 130 kyr BP Mt. Taranaki can be summarized in four main periods of activity (Alloway et al., 2005).

**(1)** ca. 130 to 14 kyr BP. Thirteen edifice collapses spread debris avalanche deposits to NE, SE and SW flanks of the current volcano (Zernack et al., 2011). The deposits from these are intercalated with debris and hyperconcentrated flow deposits (e.g. Neall, 1979; Zernack et al., 2011), and with pyroclastic deposits from explosive eruptions, which have been mapped and assigned to 20 tephra formations (e.g. Neall, 1972; Alloway et al., 1995; 2005).

**(2)** ca. 14 to 7 kyr BP. Plinian eruptions generated thick fall deposits (e.g. Alloway et al., 1995). They were contemporaneous with the earliest-dated E- and W-directed block-and-ash flow deposits (BAF) and with lahars flowing down the volcano (e.g. Neall, 1979). Warwicks Castle lavas started building the youngest volcanic edifice. Lava deposits located on the south and east of the edifice collapsed, leading to the generation of the ca. 7.5 kyr BP Opua debris avalanche (Neall, 1979; Zernack et al., 2011).

**(3)** ca. 7 kyr BP to ca. 1000 AD. Eruption of the Peters lavas (Neall, 2003) contributed to rebuilding of the edifice. Fanthams Peak was likely formed early during this stage (Stewart et al., 1996). Some of the largest plinian to sub-plinian eruptions in Mt. Taranaki's history occurred during this time. These eruptions produced at least four tephra formations distributed to SE, E, and NE of the volcano: ca. 5.4 kyr BP Tariki, ca. 4.1 kyr BP Korito, ca. 3.6 kyr BP Inglewood, and ca. 2.9-3.3 kyr BP Manganui (Whitehead, 1976; Alloway et al., 1995). Most plinian fall deposits accumulated on top of thick E- and W-directed BAF deposits. In contrast, low-explosive fallouts like ca. 2 kyr BP Maketawa Tephra and ca. 1.8 kyr BP Curtis Ridge Lithic Lapilli (Turner, 2008), are intercalated with much thinner/smaller E-distributed BAFs. The Staircase and Skeet lava flows were extruded and partially filled in the amphitheatre left by the Opua collapse (Stewart et al., 1996; Neall, 2003). The ca. 1.3 kyr BP Kaupokonui Tephra (McGlone et al., 1988) might be an explosive correlative to such effusive activity. Lava domes also erupted on the lower flanks of the volcano (e.g. The Dome, Skinner Hill, Beehives domes; Neall et al., 1986; Platz et al., 2012).

**(4)** ca. 1000 AD to present. Eruption of the Summit lavas (Stewart et al., 1996) shaped the bulk of the upper part of the present-day cone. At least five W-distributed BAF and surge units deposited ash and thin lapilli beds around proximal areas between ca. 1150-1600 AD (e.g. Newall, Waiweranui and Puniho lapilli and ashes; Druce, 1966; Neall, 1972; Alloway and Neall, 1994). The sub-plinian Burrell eruption ensued and released $3x10^6$ $m^3$ of pyroclastic density current deposits, and $3.2x10^8$ $m^3$ of fallout deposits from a 14 km column (Platz et al., 2007). It was followed by smaller explosive (e.g. ca. 1755 AD Tahurangi ash, Druce, 1966; Neall, 1972) and effusive events (e.g. ca. 1800 AD Sisters dome, Platz et al., 2012).

## Eruptive units and lithofacies

The field trip focuses on proximal deposits produced during the last 5,000 yr. These are classified into eruptive units and subunits, and include the deposits of the Korito, Inglewood, Manganui, Maketawa, Kaupokonui and Burrell Tephra formations. Evidence of significant repose periods in the volcanic activity is provided by paleosols (millimetre to centimetre scale) and deep-erosive paleochannels (in most cases correlative to lahar and fluvial deposits in ring-plain locations), forming unconformities bounding different eruptive units (Fig. 2).

To complete a lithofacies analysis of the eruptive units (Pardo et al., 2012; Kim et al., 2014); detailed field observations have been registered in sedimentary logs. Records of bed geometry, sedimentary structures (e.g. contact types, grain-size, grading, bedform and stratification, dunes, clast lenses, and syn-depositional deformational structures [e.g. impact sags]), sorting, framework (e.g. matrix- and clast-supported), componentry (e.g. pumice/scoria and lithics), and clast texture (e.g. colour, shape, crystallinity, vesicularity, and vesicle size, shape and fabric) have been made.

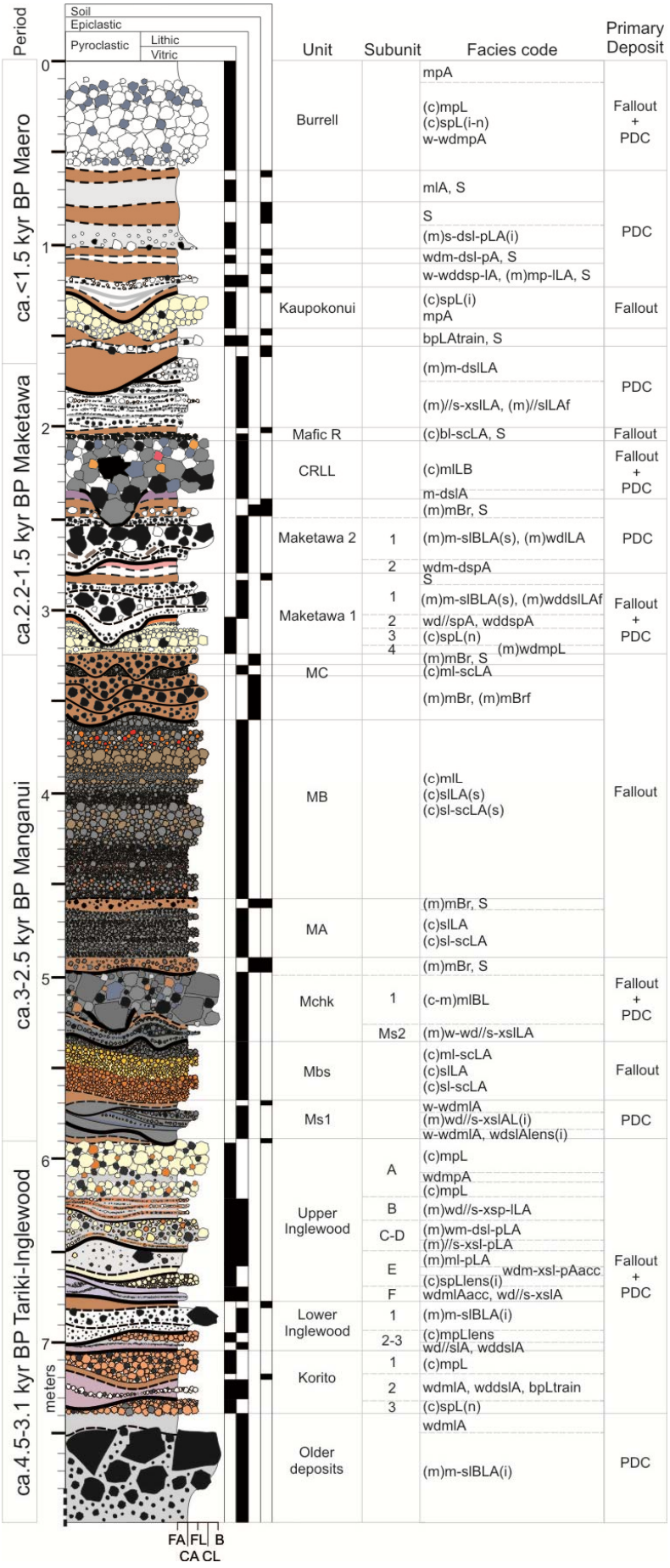


Figure 2. Composite litho-stratigraphic column of the proximal eastern sector of Mt. Taranaki (Torres-Orozco et al., in review).

A total of 16 eruptive units were identified at the eastern sector of Mt. Taranaki (Fig. 2). During this fieldtrip, we will observe and correlate some of them (Fig. 3).

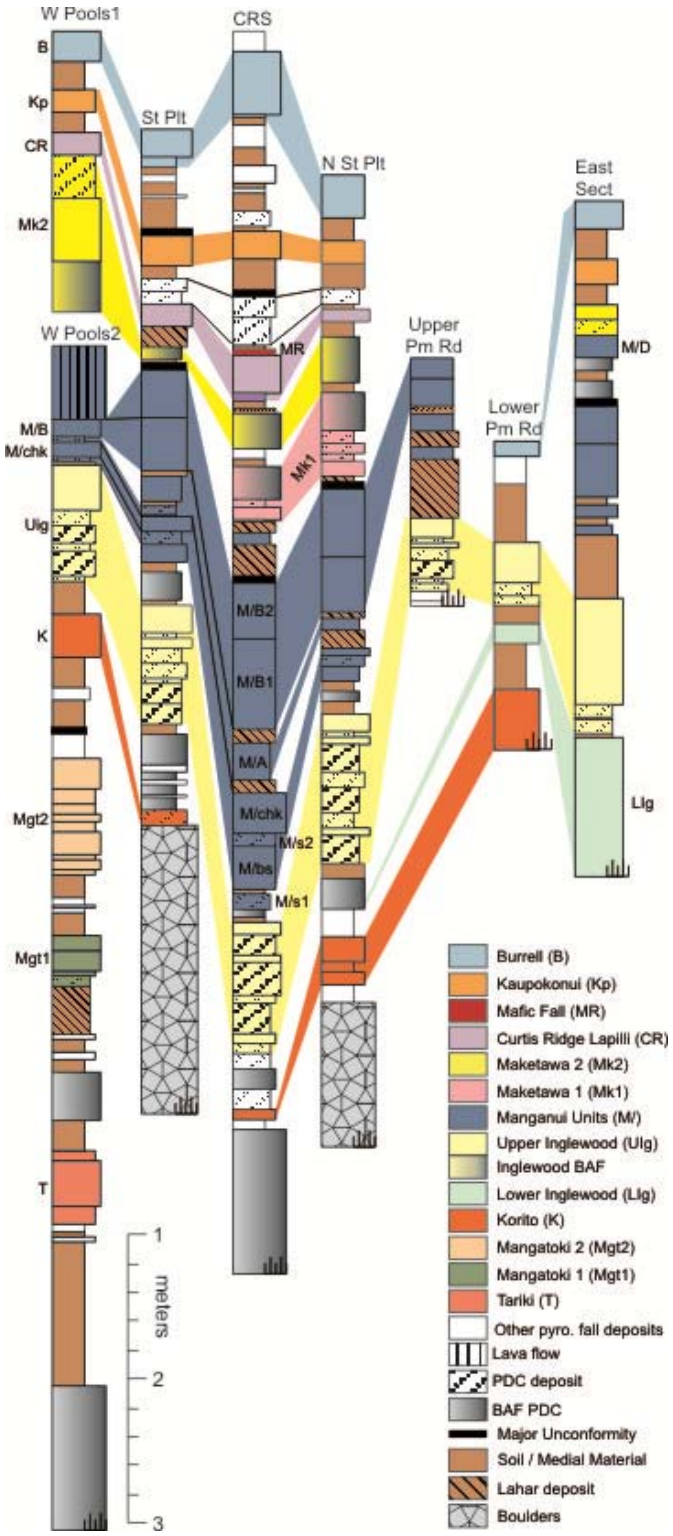


Figure 3. Stratigraphic correlation of the proximal eastern sector of Mt. Taranaki (Torres-Orozco et al., in review).

## Medial-distal deposits from swamps

Several swamps and lakes surrounding Mt Taranaki were drilled for compilation of a record of macro- and microscopic tephras. During this fieldtrip we will observe and discuss some of the cores collected, as they are critical to understanding the long-term volcanic eruption history and consequent probabilistic hazard forecasting of event onset, magnitude and style.

The use of tephra layers from medial to distal sites has been very successful in terms of high-resolution tephrochronology, because proximal deposits are often prone to erosion and burial by younger deposits. However, the application of tephrochronology is not always straightforward and requires more precise and multi-proxy approaches to develop a complete record. By investigating a broad network of coring sites and the collection of long continuous sediment sequences, we were able to provide a highly detailed tephrochronological record. These data provide an unprecedented view into the temporal variation in eruptive dynamics of Mt Taranaki, including regular changes in geochemistry, and eruption frequency and magnitude. Tephra dispersal patterns caused by shifting paleo-wind direction can also be reconstructed and used to build robust probabilistic hazard models for ash fall impacts. The results combined with those from other tephra sites promise to provide a fundamental contribution to the understanding of andesite magmatic systems and the long-term eruption behaviour of Mt Taranaki.

# STOP 1: Wilkies Pools section 1

View of Maketawa 1 and Maketawa 2 eruptive units and subunits (Fig. 2). Deposits show facies varying in framework (clast- and matrix-support), stratification (massive, parallel, and cross-stratification), sorting (sorted and poorly sorted), and componentry (pumice/lithic ratio). Matrix-supported deposits (m) at this section tend to wedge (wd), develop diffuse laminar stratification (ds) with distance, and may include faint imbricated clasts (f). They mostly contain inversely graded (i), andesite lithic lapilli- and block-sized, subangular to subrounded clasts, and few pumice lapilli. Moreover, (m) deposits exhibit sharp and highly erosive lower contacts, partially destroying older deposits. Clast-supported deposits (c) are continuous and mantle the pre-existing topography. They are better sorted and vary in between massive and strong parallel symmetric stratifications. Friable, subangular pumice lapilli is the main component of the (m) facies of Maketawa 2; although, other (c) facies deposits may contain more lithics.

At Wilkies Pools, Maketawa 2 was deposited along a channel. The pre-existing topography affected the deposition of the (m) subunit, making it to expand and wedge to produce “highly-concentrated” (c) lenses, develop few clast bedding, imbrication, and diffuse ash and lapilli laminations. Such characteristics correspond to a dense pyroclastic density current (PDC). Because of the high and relatively homogeneous lithic content, and the inverse stratification which includes blocks on the top of the deposit due to dispersive pressure, the PDC was likely produced after the eruption and collapse of a dome on top of the crater of Mt. Taranaki (block-and-ash flow). The PDC might have eroded and incorporated deposits of Maketawa 1. Subsequently, the Maketawa 2 (c) subunit erupted and deposited pumice lapilli falling from an eruptive column and mantling the topography earlier created by the (m) subunit. Such mechanism enables sorting of clasts, parallel stratification and grain-size grading according to column energy fluctuations.

## STOP 2: Wilkies Pools section 2

From base to top, view of ca. <5 kyr BP Tariki, Mangatoki, Korito, Upper Inglewood, and Manganui eruptive units, older than Maketawa units (Fig. 2). The focus at this section places on Upper Inglewood and Manganui units, with the aim of identifying lateral variations along next eastern sections. With the exception of Manganui units, most deposits resemble either marginal or near-marginal facies of distribution; therefore, weathering and soil development have modified many primary structures.

At Wilkies Pools 2, Upper Inglewood unit exhibits three apparent subunits. Two of them show (m), wedging, massive to diffuse stratified to parallel/cross-stratified, and poorly sorted facies, in contrast with the (c), mantling, massive and better sorted top subunit. Both (m) deposits keep relatively even contents of subrounded to subangular, fine lapilli-sized pumice and lithic clasts, whereas the (c) top is rich in subangular pumice lapilli and less angular to subangular lithics.

Two eruptive units of the Manganui period are visible on the upper part of the section: Manganui chonky (Mchk) and part of Manganui B (MB; Fig. 2). Mchk comprises a lower, wedging and waving, diffused laminar stratified subunit (Ms2) of bluish ash supporting few lithic lapilli; and an upper (c), mantling, massive to stratified deposit of loose, black lithic lapilli. The (c) facies deposit also includes block-sized lithic ballistics impacting and deforming the top of Ms2. MB is separated from Mchk by another wedging-waving, diffused laminar stratified subunit (Ms3); and consists of (c), loose, massive black to grey lithic lapilli; however, the top of this unit was eroded.

Like in section 1, here (m)-stratified facies correspond to PDC deposits; yet in this case, because of the much higher content of fine particles supporting less lapilli clasts and yielding a more developed stratification in both, Inglewood and Manganui units, they are interpreted as the result of energetic, dilute to fully dilute, turbulent PDCs. Similarly, (c) deposits were produced by eruptive columns transporting pyroclasts into the atmosphere which afterwards fall and mantle the surface. Though, Upper Inglewood fall deposit portrays marginal facies of deposition, whilst Mchk and MB deposits, at this section, seem to correspond with the main-axis of distribution.

## STOP 3: Stratford Plateau section

Recognition of lateral transitions of PDC and fallout deposits from Upper Inglewood, Manganui, and Maketawa 2 eruptive units and subunits. The variety of lithofacies increases, yet (c)- and (m)-massive to stratified facies are still defining.

The six subunits of Upper Inglewood (A to F; Fig. 2) become clear at Stratford Plateau section. From base to top, F-B show either (m)-wedging and waving, massive to stratified, lithic and pumice ash and lapilli facies, or only wedging and waving, massive to diffuse stratified, lithic and pumice ash facies. Both cases have been interpreted as PDC deposits with differences in turbulence and dilution. Subunit A correlates with the (c)-massive, mantling, subangular pumice lapilli deposit of Wilkies Pools section 2. Though, at this section, a wedging, massive pumice ash was deposited in the middle of subunit A; and was interpreted as a confined PDC deposit produced by a small column-collapse.

All units that constitute the Manganui eruptive period (Fig. 2) are also recognizable at Stratford Plateau section. Most of them portray (c)-massive to stratified, mantling facies of loose, subangular

lithic dense and vesicular (scoria-like) lapilli (Fig. 2). They were interpreted as fall deposits produced by an explosive eruption column. Some wedging, parallel to cross-stratified, and diffuse stratified facies deposits of lithic ash (Ms2 and Ms3) were interpreted as diluted to fully-diluted (surge) PDC deposits. Ms2 contains small pieces of charcoal that support high temperatures of deposition.

Maketawa 2 becomes barely noticeable as deposits thin out at this section, far from the channel-facies of Wilkies Pools section 1. Here, deposits develop wedging, massive to parallel and cross-stratified lithic-pumice ash and lapilli facies closer to overbank-PDC conditions.

## STOP 4: Stratford Plateau car-park and Curtis Ridge section

Curtis Ridge constitutes one of the best sections to study thick deposits (yet not the thickest) of the largest Manganui eruption (MB unit), and to observe complete sedimentary structures of subunits E-F within Upper Inglewood (Fig. 2). The (c) massive to stratified pumice lapilli facies of Kaupokonui and Burrell Lapilli within their corresponding eruptive units (Fig. 2) can be also recognized.

Upper Inglewood subunits A-D become massive and likely mixed. This is probable due to the immediacy with the source of the eruption since Curtis Ridge is one of the most proximal sections. However, subunits can be still recognized. Subunits E and F expand and exhibit a variety of lithofacies (Fig. 2). Subunit E can be divided into (m)-massive, lithic-pumice lapilli and ash; and wedging, massive to cross-stratified, lithic-pumice ash facies, bearing few accretionary lapilli and supporting (c)-stratified, pumice lapilli lenses. Each facies denotes different PDC processes. The first case indicates a slightly dense to dilute, turbulent PDC; while the second corresponds to a more dilute and turbulent PDC, which interacted with either steam or water to become indurated and produce accretions. Facies of subunit F are very similar to E, suggesting comparable PDC-processes.

MB comprises (c)-massive to stratified (symmetric), lithic dense to vesicular (scoria-like), loose, black to grey-brownish lapilli and ash facies, defining three main explosive pulses. The first two pulses vary from symmetric graded to massive thick deposits, whilst the top pulse is strongly stratified, making parallel massive thick and thin beds. Such variations were interpreted as a plinian eruption column fluctuating into a sub-plinian plume at the end of the explosive event.

At Curtis Ridge it is possible to observe deposits of both Maketawa 1 and 2 units. Both units comprise (m) wedging, massive to parallel and diffuse stratified pumice and/or lithic ash and lapilli; and (m) massive to stratified lithic blocks, lapilli, and ash; (Fig. 2). These facies correspond to PDC deposits of different nature. The first concerns to slightly dense to fully dilute surge-PDCs related to either a co-ignimbrite (lithic, dilute part of a block-and-ash flow), or to a small, dense column-collapse (pumice PDC). The second corresponds to a dense block-and-ash flow, like in Wilkies Pools section 1, but in overbank-facies, as suggested by the more developed stratification and the presence of diluted facies. Maketawa 1 also includes (c) normal-graded, pumice lapilli facies, proper of a fall deposit.

Explanation and discussion of medial-distal pyroclastic deposits drilled in swamps will be carried out at the car-park.

## STOP 5: New Stratford Plateau section

View of longitudinal-facies transition in deposits of Upper Inglewood, Manganui and Maketawa units with respect to Curtis Ridge section. Lower Inglewood and Korito eruptive units can be also identified. Upper Inglewood subunits C-D likely transit into syn-eruptive, fluvial-reworking facies, bounded in between primary deposition facies of subunits E and B. PDC subunits of both Maketawa eruptions become more diluted and stratified.

## STOP 6: Upper Pembroke Road Section

Observation of proximal-longitudinal thinning out and stratification of Manganui and Upper Inglewood deposits.

## STOP 7: Lower Pembroke Road Section

Observation of medial-longitudinal thinning out, weathering, and edafization of Manganui, Upper Inglewood, Lower Inglewood and Korito units.

## References


Alloway BV and Neall VE (1994) Late Quaternary Volcaniclastic Stratigraphy of Central & North-east Taranaki. In: Briggs R and Moon V (eds) 1994 Annual Conference. Field Trip Guides, Geological Society of New Zealand Miscellaneous Publication 80B: 97-126

Alloway B, Neall VE and Vucetich CG (1995) Late Quaternary (post 28,000 year B.P.) tephrostratigraphy of northeast and central Taranaki, New Zealand. Journal of the Royal Society of New Zealand 25, 385-458

Alloway B, Mc Comb P, Neall V, Vucetich C, Gibb J, Sherburn S, and Stirling M (2005) Stratigraphy, age, and correlation of voluminous debris-avalanche events from an ancestral Egmont Volcano: implications for coastal plain construction and regional hazard assessment. Journal of the Royal Society of New Zealand 35, 229-267

Carey S and Sigurdsson H (1987) Temporal variations in column height and magma discharge rate during the A.D. 79 eruption of Vesuvius. Geological Society of America Bulletin 99: 303-314

Carn SA, Pallister JS, Lara L, Ewert JW, Watt S, Prata AJ, Thomas RJ, Villarosa (2009) The unexpected awakening of Chaitén Volcano, Chile. EOS Transactions, AGU 90 (24): 205-206

Cronin SJ, Lube G, Dayudi DS, Sumarti S, Subrandriyo S and Surono (2013) Insights into the October-November 2010 Gunung Merapi eruption (Central Java, Indonesia) from the stratigraphy, volume and characteristics of its pyroclastic deposits. J. Volcanol. Geoth. Res. 261: 244-259

Druce AP (1966) Tree-ring dating of recent volcanic ash and lapilli, Mt Egmont. New Zealand Journal of Botany 4, 3-41

Gudmundsson M and Pedersen R (2010) Eruptions of Eyjafjallajokull Volcano, Iceland. Eos 91 (21): 190-191

Kim GB, Cronin SJ, Yoon WS, and Sohn YK (2014) Post 19 ka B.P. eruptive history of Ulleung Island, Korea, inferred from an intra-caldera pyroclastic sequence. Bulletin of Volcanology 76:802

Langmann B, Folch A, Hensch M and Matthias V (2012) Volcanic ash over Europe during the eruption of Eyjafjallajokull on Iceland, April-May 2010. Atmospheric Environment 48: 1-8

Manville V, Németh K, Kano K (2009). From source to sink: a review of three decades of progress in the understanding of volcaniclastic processes, deposits, and hazards. Sedimentary Geology 220: 136-161

McGlone MS, Neall VE and Clarkson BD (1988) The effect of recent volcanic events and climatic changes on the vegetation of Mt Egmont (Mt Taranaki), New Zealand. New Zealand Journal of Botany 26, 123-144.

Neall VE and Alloway BE (2004) Quaternary Geological Map of Taranaki. Institute of Natural Resources, Massey University, Soil and Earth Sciences Occasional Publication 4.

Neall VE, Stewart RB and Smith IEM (1986) History and petrology of the Taranaki volcanoes. In: Smith IEM (ed.) Late Cenozoic volcanism. Royal Society of New Zealand Bulletin 23, 251-263.

Neall VE (1972) Tephrochronology and tephrostratigraphy of western Taranaki (N108-109), New Zealand. New Zealand Journal of Geology and Geophysics 15, 507-557.

Neall VE (1979) Sheets P19, P20, and P21. New Plymouth, Egmont and Manaia. 1st ed. Geological map of New Zealand 1:50,000. 3 maps and notes. New Zealand Department of Scientific and Industrial Research. Wellington.

Neall VE (2003) The volcanic history of Taranaki. Institute of Natural Resources, Massey University, Soil & Earth Sciences Occasional Publication 2.

Pardo N, Cronin SJ, Palmer A, Németh K (2012a) Reconstructing the largest explosive eruptions of Mt. Ruapehu, New Zealand: lithostratigraphic tools to understand subplinian-Plinian eruptions at andesitic volcanoes. Bull Volcanol 74: 617-640.

Pardo N, Cronin SJ, Palmer A, Procter J, Smith I (2012b). Andesitic Plinian eruptions at Mt. Ruapehu: quantifying the uppermost limits of eruptive parameters. Bull Volcanol 74: 1161-1185.

Platz T, Cronin SJ, Cashman KV, Stewart RB, Smith IEM (2007) Transitions from effusive to explosive phases in andesite eruptions-A case-study from the AD 1655 eruption of Mt. Taranaki, New Zealand. J. Volcanol. Geotherm. Res. 161: 15-34

Platz T, Cronin SJ, Procter JN, Neall VE and Foley SF (2012) Non-explosive dome-forming eruptions at Mt. Taranaki, New Zealand. Geomorphology 136: 15-30

Stewart RB, Price RC, Smith IEM (1996) Evolution of high-K arc magma, Egmont volcano, Taranaki, New Zealand: evidence from mineral chemistry. J. Volcanol. Geotherm. Res. 74: 275-295

Tilling RI, Topinka L and Swanson DA (1990) The Eruptions of Mount St. Helens: Past, Present, and Future. USGS Information Publication.

Turner MB (2008) Eruption cycles and magmatic processes at a reawakening volcano, Taranaki, New Zealand. PhD thesis, Massey University, Palmerston North.

Whitehead SJ (1976) Granulometric studies on selected tephra eruptions, North Island, New Zealand. Unpublished Honours Dissertation, Massey University, Palmerston North.

Wilson CJN, Houghton BF, McWilliams MO, Lanphere MA, Weaver SD, Briggs RM (1995) Volcanic and structural evolution of Taupo Volcanic Zone, New Zealand: a review. J. Volcanol. Geotherm. Res. 68: 1-28

Wilson CJN (1997) Emplacement of Taupo ignimbrite. Nature scientific correspondence 385: 306-307

Zernack AV, Cronin SJ, Neall VE and Procter JN (2011) A medial to distal volcaniclastic record of an andesite stratovolcano: Detailed stratigraphy of the ring-plain succession of south-west Taranaki, New Zealand. International Journal of Earth Sciences 100, 1936-1966.